

1 Supplement for manuscript

2 **Real-time measurements of aerosols in Seoul, Korea using a**  
3 **high-resolution aerosol mass spectrometer (HR-AMS):**  
4 **insights into the sources and processing of organic and**  
5 **inorganic aerosols during wintertime**

6 **Hwajin Kim<sup>1,2</sup>, Qi Zhang<sup>3,4\*</sup>, Gwi-Nam Bae<sup>1,2</sup>, Jin Young Kim<sup>1,2</sup>, Seung Bok Lee<sup>1,2</sup>**

7 [1] Center for Environment, Health and Welfare Research, Korea Institute of Science and  
8 Technology, Seoul, Korea

9 [2] Department of Energy and Environmental Engineering, University of Science and  
10 Technology, Daejeon, Korea

11 [3] Department of Environmental Toxicology, University of California, Davis, CA 95616, USA

12 [4] Department of Environmental Science and Engineering, Fudan University, Shanghai, China.

13

14 \*Corresponding author: Qi Zhang

15 Department of Environmental Toxicology, University of California 1 Shields Avenue, Davis,  
16 California 95616

17 Phone: (530)-752-5779

18 Email: [dkwzhang@ucdavis.edu](mailto:dkwzhang@ucdavis.edu)

19

20

21

22

23

24

25

26  
27  
28  
29  
30  
31  
32  
33  
34  
35  
36  
37  
38  
39  
40  
41  
42  
43  
44  
45  
46  
47  
48  
49  
50

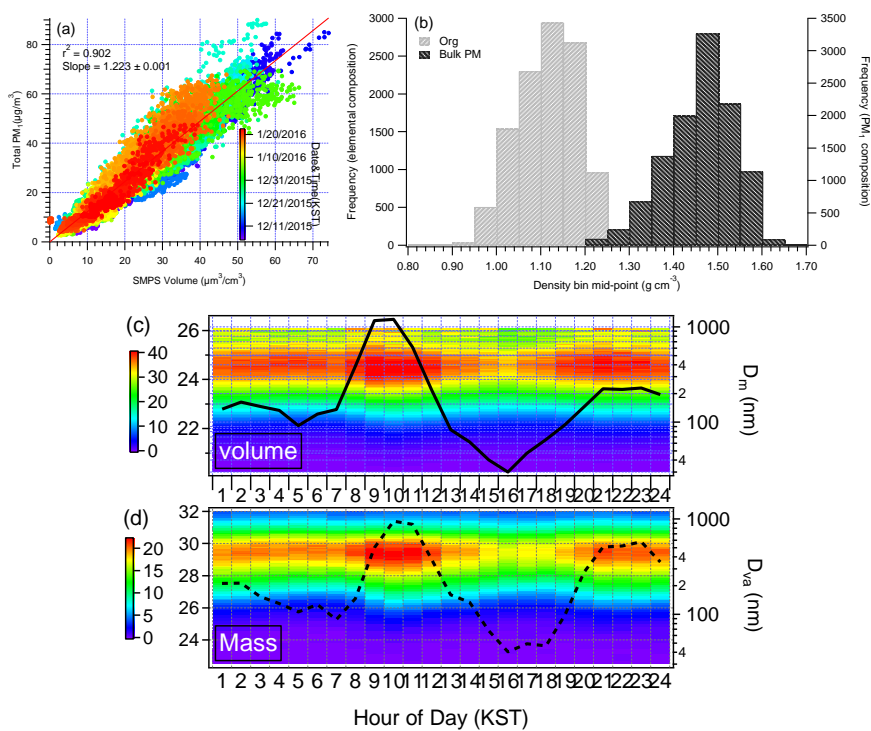


**Figure S1.** (a) Scatter plot of the total PM<sub>1</sub> mass (NR-PM<sub>1</sub> plus BC) versus SMPS volume, where the NR-PM<sub>1</sub> has been corrected using a time- and composition-dependent collection efficiency (Middlebrook et al., 2012); (b) histogram of organic density calculated measured elemental ratios (Kuwata et al., 2012), averaging 1.12 g cm<sup>-3</sup> and bulk aerosol density estimated from the measured chemical composition in this study (Zhang et al., 2005), averaging 1.46 g cm<sup>-3</sup>. (c) Diurnal variations of the size distribution of volume from the SMPS (in mobility diameter,  $D_m$ ) and (d) NR-PM<sub>1</sub> mass from the AMS (in vacuum aerodynamic diameter,  $D_{va}$ ).

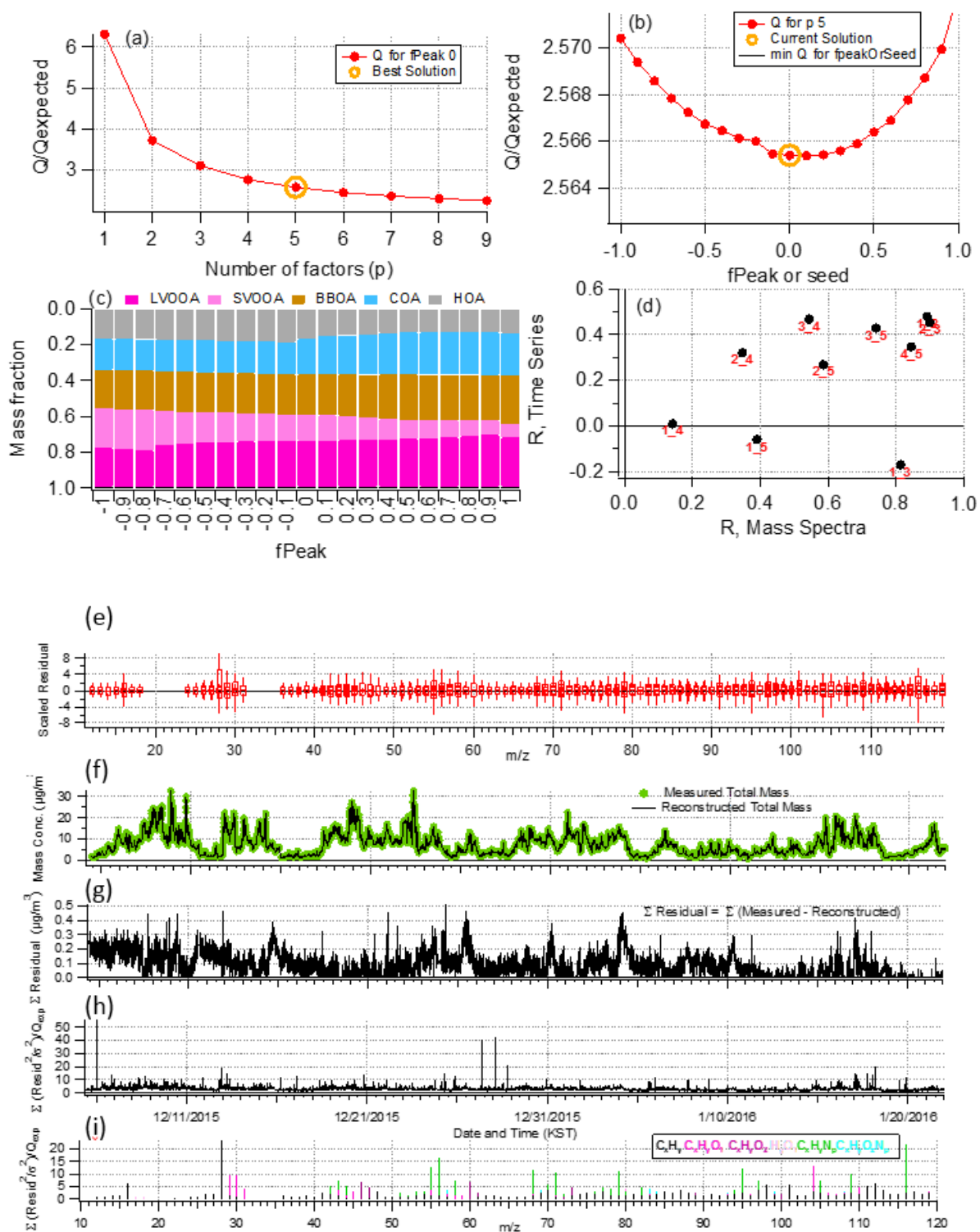
51 **Table S1.** Comparison of the O/C, H/C, and OM/OC ratios of total OA and the six OA factors  
 52 identified from PMF analysis calculated using the Aiken-Ambient method (Aiken et al., 2008) and  
 53 the improved Canagaratna-Ambient method (Canagaratna et al., 2015).

54

Species	Ratio	Aiken-Ambient	Canagaratna-Ambient
OA	O/C	0.29	0.37
	H/C	1.62	1.79
	OM/OC	1.54	1.67
HOA	O/C	0.05	0.06
	H/C	2.04	2.21
	OM/OC	1.24	1.27
COA	O/C	0.11	0.14
	H/C	1.76	1.89
	OM/OC	1.30	1.36
BBOA	O/C	0.26	0.34
	H/C	1.56	1.74
	OM/OC	1.49	1.61
SVOOA	O/C	0.43	0.56
	H/C	1.70	1.90
	OM/OC	1.74	1.94
LVOOA	O/C	0.52	0.68
	H/C	1.42	1.61
	OM/OC	1.84	2.07

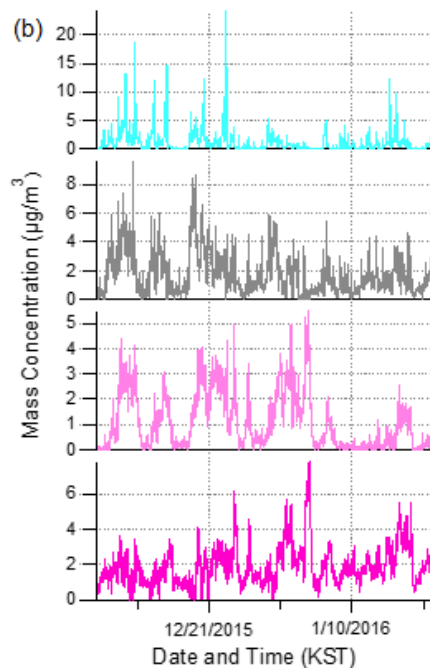
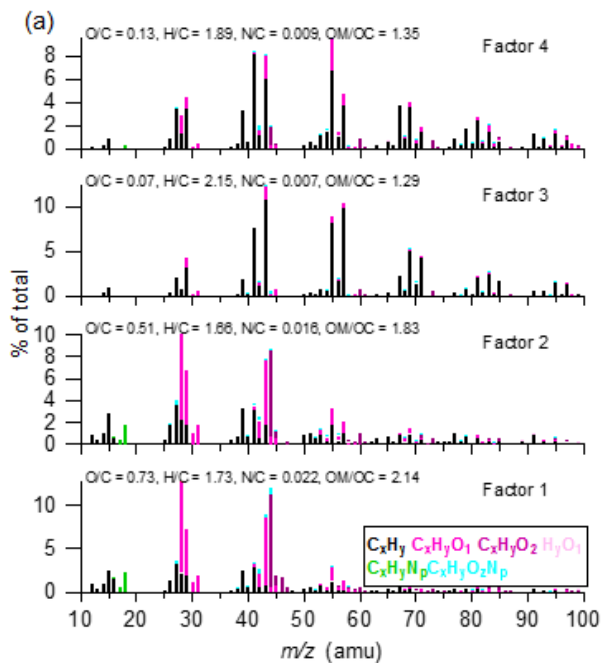
55

56  
57  
58  
59  
60  
61  
62  
63  
64  
65  
66  
67  
68  
69  
70  
71  
72  
73  
74  
75  
76  
77

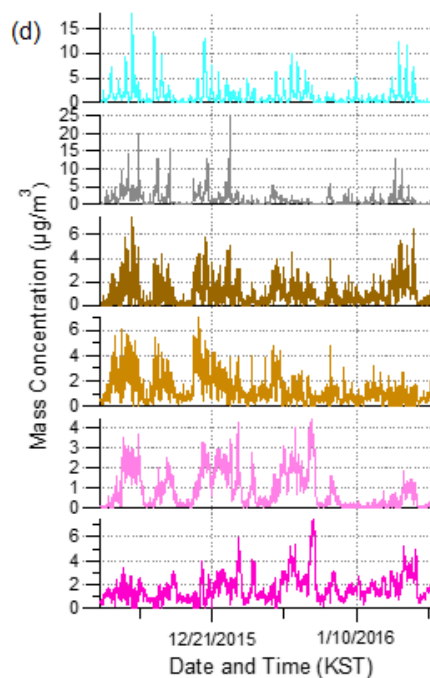
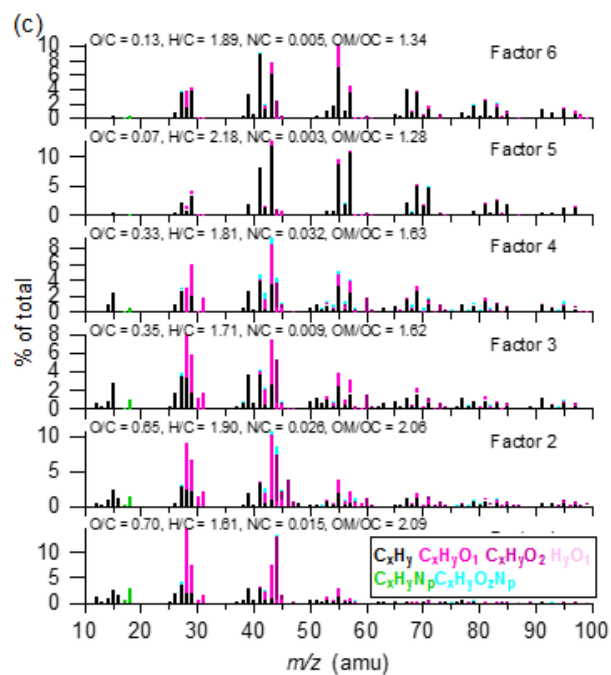


78 **Figure S2.** Summary of the key diagnostic plots of the chosen 5-factor solution from PMF analysis  
79 of the organic aerosol fraction: **(a)**  $Q/Q_{exp}$  as a function of the number of factors ( $p$ ) explored in  
80 PMF analysis, with the best solution denoted by the open orange circle. Plots **b-i** are for the chosen  
81 solution set, containing 5 factors: **(b)**  $Q/Q_{exp}$  as a function of fPeak; **(c)** mass fractional contribution  
82 to the total OA mass of each of the PMF factors, including the residual (in black), as a function of  
83 fPeak; **(d)** Pearson's  $r$  correlation coefficient values for correlations among the time series and  
84 mass spectra of the PMF factors. Here, 1 = LV-OOA, 2 = SV-OOA, 3 = BBOA, 4 = HOA, 5 = COA;  
85 **(e)** box and whiskers plot showing the distributions of scaled residuals for each  $m/z$ ; **(f)** time series  
86 of the measured organic mass and the reconstructed organic mass from the sum of the five OA  
87 factors; **(g)** time series of the variations in the residual (= measured – reconstructed) of the fit; **(h)**  
88 the  $Q/Q_{exp}$  for each point in time; **(i)** the  $Q/Q_{exp}$  values for each fragment ion.

89  
90  
91  
92  
93  
94  
95  
96  
97  
98  
99



100  
101  
102  
103  
104  
105  
106  
107  
108  
109  
110  
111  
112



113 **Figure S3.** Overview of two other solution sets from PMF analysis: **(a)(b)** High resolution mass  
114 spectra and time series of the different OA factors from the 4-factor solution; **(c)(d)** High resolution  
115 mass spectra and time series of the different OA factors from the 6-factor solution. The mass  
116 spectra are colored by different ion families and the time series are colored by possible factor  
117 sources (grey = HOA, blue = COA, brown = BBOA, pink = OOA). See Sect. 2.3.2 in the main  
118 manuscript for a discussion on these solution sets.

119

120

121

122

123

124

125

126

127

128

129

130

131

132

133

134

135

136

137

138

139

140

141

142

143

144

145

146

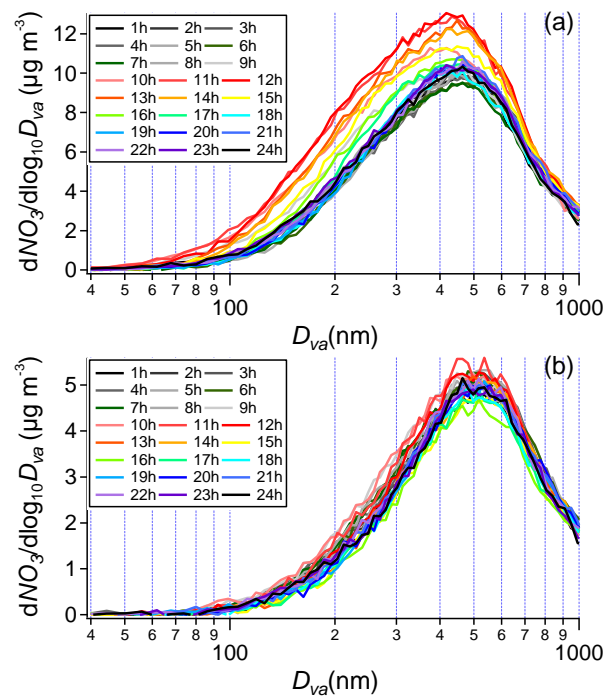
147

148

149

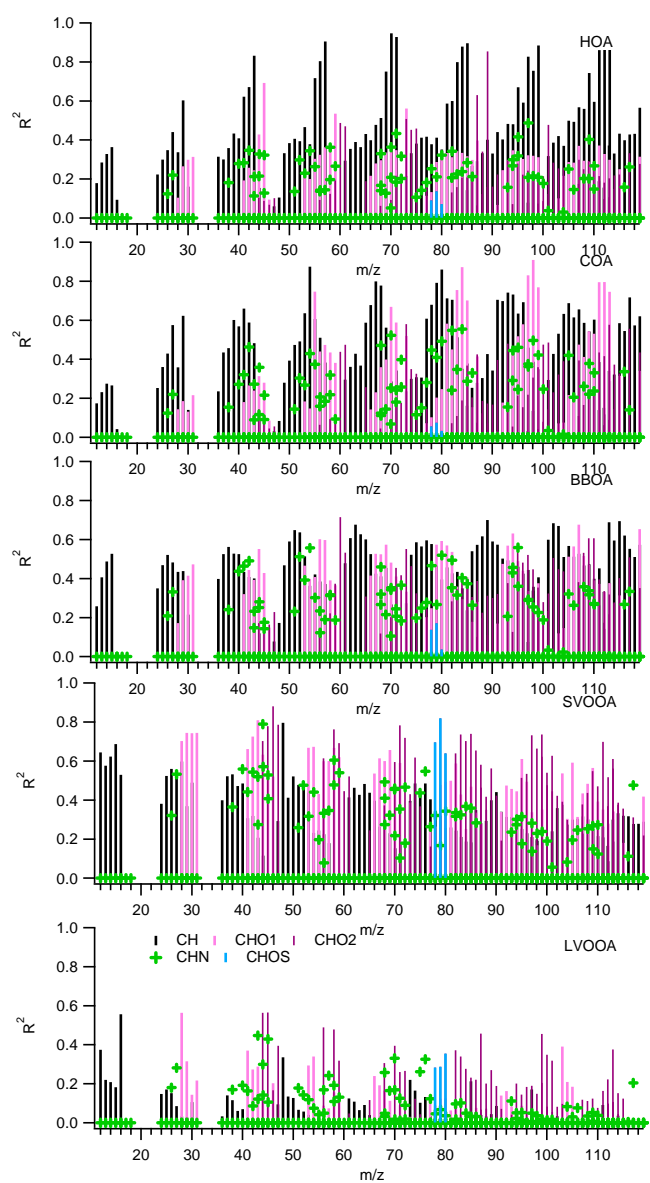
150 **Figure S4.** Hourly averaged mass-based size distributions of (a) nitrate and (b) sulfate during  
151 the entire period. Hour shown at legend indicate the diurnal hour of the day.

152





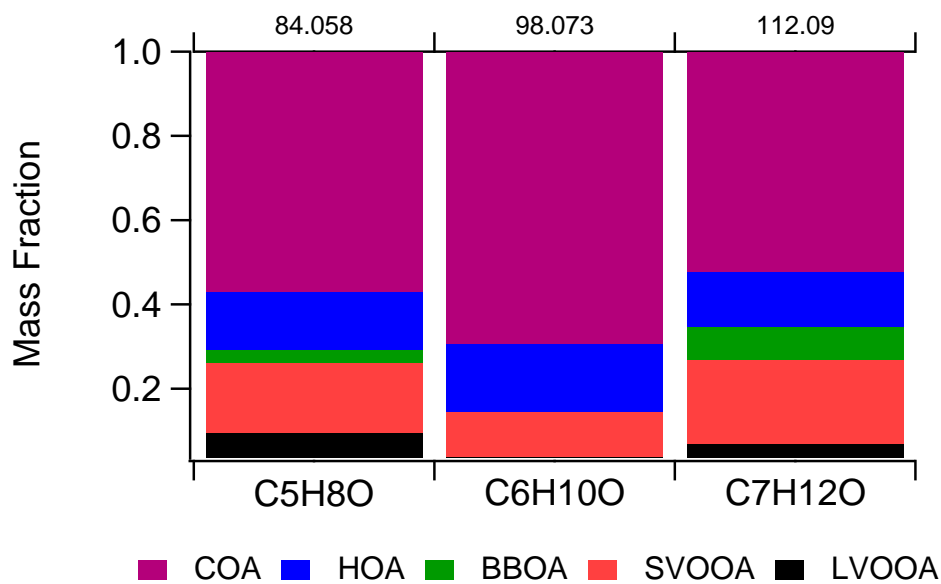
153  
154  
155  
156  
157  
158  
159  
160  
161  
162  
163  
164  
165  
166  
167  
168  
169  
170



171 **Figure S5.** Correlations between five OA factors and HRMS ions that are segregated into five  
172 categories ( $C_xH_y^+$ ,  $C_xH_yO^+$ ,  $C_xH_yO_2^+$ ,  $C_xH_yN_p^+$  and  $C_xH_yO_zS_q^+$ ).

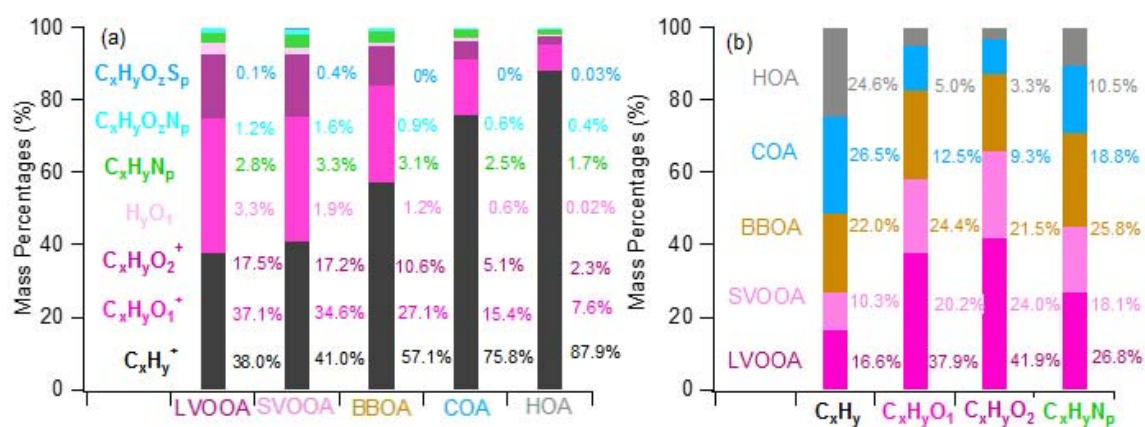
173  
174  
175

176



177

178 **Figure S6.** Mass fractional contribution of the five OA factors from PMF analysis to various ions  
179 that are relevant to COA tracers.



180  
 181 **Figure S7.** (a) Average mass fractional contributions of seven ion families to each of the OA  
 182 factors and (b) Average mass fractional contributions of five OA factors to 4 each ion families

183  
 184  
 185  
 186  
 187  
 188  
 189  
 190  
 191  
 192  
 193  
 194  
 195  
 196

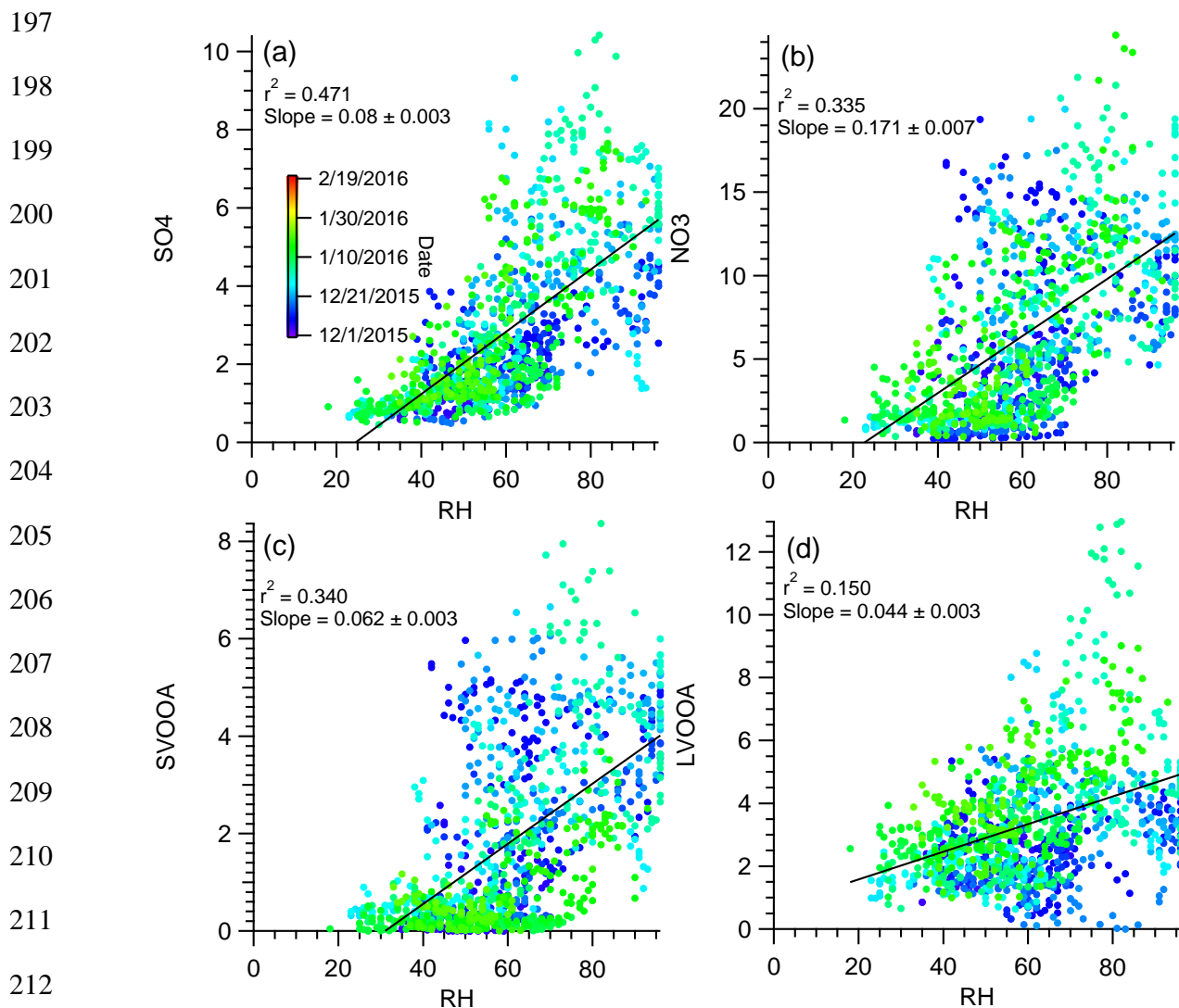
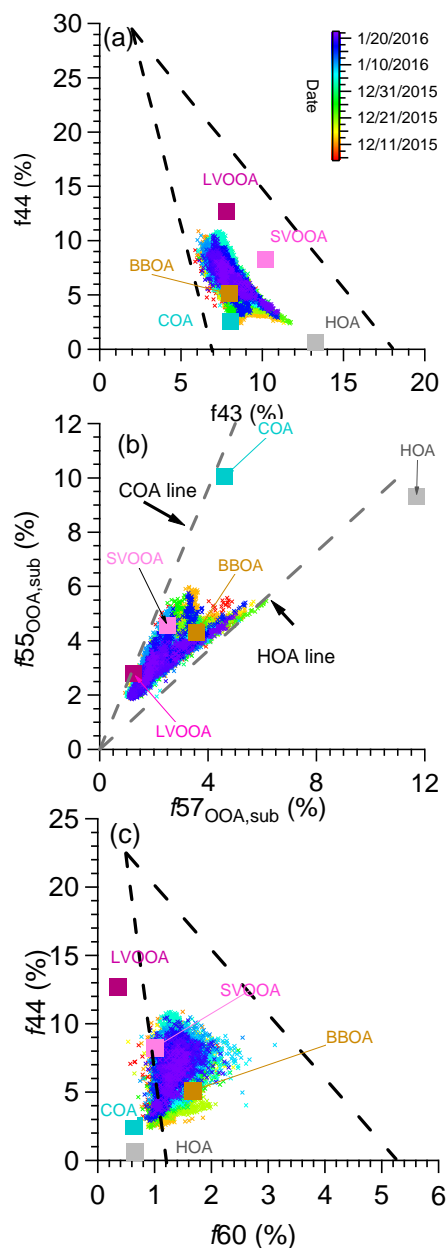


**Figure S8.** Scatterplot between inorganic compounds: (a) sulfate (b) nitrate which can be formed by aqueous phase reaction under high RH versus RH; and (c) SV-OOA and (d) LV-OOA which OA source that can be formed secondarily under high RH.

221  
 222  
 223  
 224  
 225  
 226  
 227  
 228  
 229  
 230  
 231  
 232  
 233  
 234  
 235  
 236  
 237  
 238  
 239  
 240



241 **Figure S9.** Triangular plots of (a)  $f_{44}$  versus  $f_{43}$  and (b)  $f_{44}$  versus  $f_{60}$  (c)  $f_{55,OOA,sub}$  versus  $f_{57,OOA,sub}$   
 242  $_{sub}$  for the five OA factors and all of the measured OA data (dots), colored by the time of the day.  
 243  $f_{43}, f_{44}$ , and  $f_{60}$  are the ratios of the organic signal at  $m/z = 43, 44$ , and  $60$  to the total organic signal  
 244 in the component mass spectrum, respectively.  $f_{55,OOA,sub}$  and  $f_{57,OOA,sub}$  are the ratios of the  
 245 organic signal at  $m/z 55, 57$  after subtracting the contributions from SV-OOA and LV-OOA  
 246 (e.g.,  $f_{55,OOA,sub} = m/z 55 - m/z 55_{SV-OOA} - m/z 55_{LV-OOA}$  ;  $f_{57,OOA,sub} = m/z 57 - m/z 57_{SV-OOA} - m/z 57_{LV-}$   
 247  $_{OOA}$ )

248

249

250

251

252

253

254

255

256

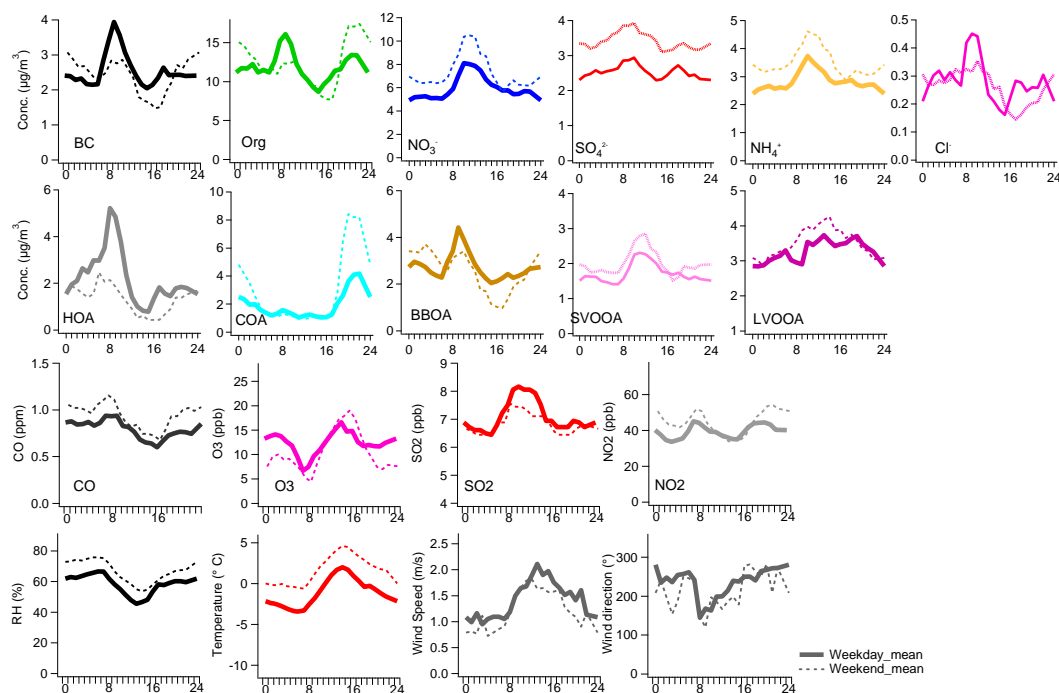
257

258

259

260

261



262 **Figure S10.** Average diurnal profiles for weekdays (Tuesday to Friday) and weekends (Sunday)

263 for the PM<sub>1</sub> species measured by the aerosol mass spectrometer (AMS) and multi angle

264 absorption photometer (MAAP) (top row), the five OA factors identified from the PMF analysis

265 (second row from the top), various gas phase species (middle row), and various meteorological

266 parameters (bottom row). In this Figure, weekdays were considered to be from Tuesday to

267 Friday, and weekends were only with Sunday. The exclusion of Monday and Saturday was to

268 reduce potential carryover effect as some species, such as nitrate, is possibly influenced by

269 emissions from the previous day (e.g., NO<sub>x</sub>). For comparisons, the results from the classification

270 of weekdays as Monday to Friday and weekends as Saturday and Sunday are reported in Fig.

271 S11.

272

273

274

275

276

277

278

279

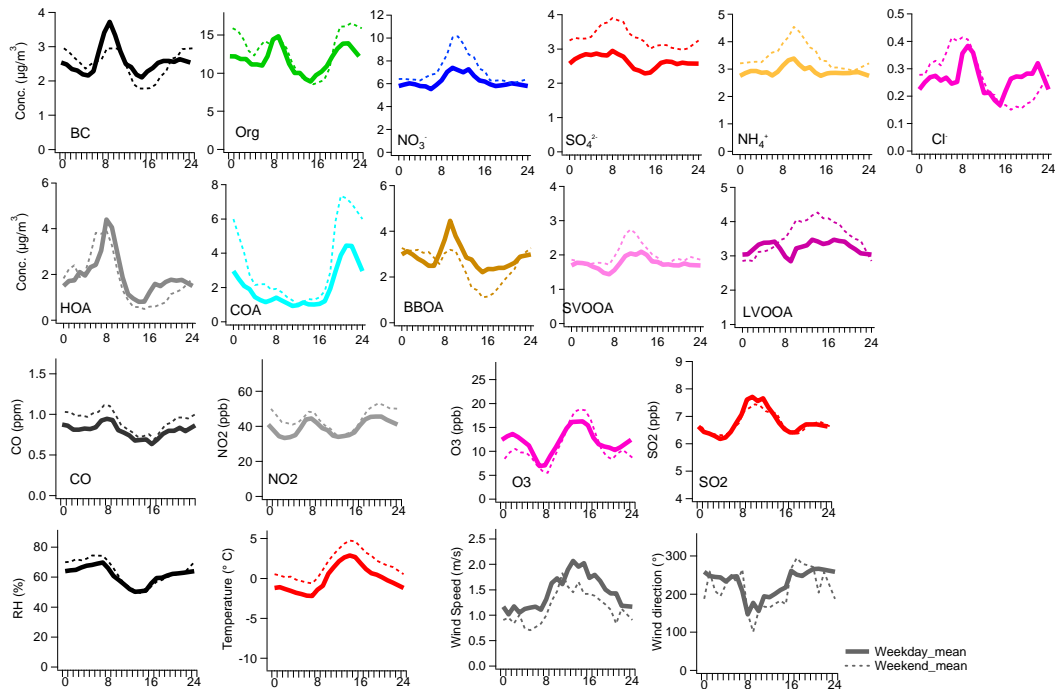
280

281

282

283

284



285

286

287 **Figure S11.** Average diurnal profiles for weekdays (Monday to Friday) and weekends (Saturday,  
288 Sunday) for the PM<sub>1</sub> species measured by the aerosol mass spectrometer (AMS) and multi angle  
289 absorption photometer (MAAP) (top row), the five OA factors identified from the PMF analysis  
290 (second row from the top), various gas phase species (middle row), and various meteorological  
291 parameters (bottom row).

292

293

294

295

296

297 **References**

298

299 Aiken, A. C., Decarlo, P. F., Kroll, J. H., Worsnop, D. R., Huffman, J. A., Docherty, K. S., Ulbrich, I. M.,  
300 Mohr, C., Kimmel, J. R., Sueper, D., Sun, Y., Zhang, Q., Trimborn, A., Northway, M., Ziemann, P. J.,  
301 Canagaratna, M. R., Onasch, T. B., Alfarra, M. R., Prevot, A. S. H., Dommen, J., Duplissy, J.,  
302 Metzger, A., Baltensperger, U., and Jimenez, J. L.: O/C and OM/OC ratios of primary, secondary, and  
303 ambient organic aerosols with high-resolution time-of-flight aerosol mass spectrometry, *Environmental*  
304 *Science & Technology*, 42, 4478-4485, 10.1021/es703009q, 2008.

305 Canagaratna, M. R., Jimenez, J. L., Kroll, J. H., Chen, Q., Kessler, S. H., Massoli, P., Hildebrandt Ruiz,  
306 L., Fortner, E., Williams, L. R., Wilson, K. R., Surratt, J. D., Donahue, N. M., Jayne, J. T., and  
307 Worsnop, D. R.: Elemental ratio measurements of organic compounds using aerosol mass  
308 spectrometry: characterization, improved calibration, and implications, *Atmospheric Chemistry and*  
309 *Physics*, 15, 253-272, 10.5194/acp-15-253-2015, 2015.

310 Kuwata, M., Zorn, S. R., and Martin, S. T.: Using Elemental Ratios to Predict the Density of Organic  
311 Material Composed of Carbon, Hydrogen, and Oxygen, *Environmental Science & Technology*, 46,  
312 787-794, 10.1021/es202525q, 2012.

313 Middlebrook, A. M., Bahreini, R., Jimenez, J. L., and Canagaratna, M. R.: Evaluation of Composition-  
314 Dependent Collection Efficiencies for the Aerodyne Aerosol Mass Spectrometer using Field Data,  
315 *Aerosol Science and Technology*, 46, 258-271, 10.1080/02786826.2011.620041, 2012.

316 Zhang, Q., Canagaratna, M. R., Jayne, J. T., Worsnop, D. R., and Jimenez, J. L.: Time- and size-resolved  
317 chemical composition of submicron particles in Pittsburgh: Implications for aerosol sources and  
318 processes, *Journal of Geophysical Research-Atmospheres*, 110, 10.1029/2004jd004649, 2005.

319

320